JOURNAL OF THEORETICAL AND APPLIED MECHANICS
49, 1, pp. 187-208, Warsaw 2011

SIMULATION AND OPTIMISATION OF THE STEERING KICKBACK PERFORMANCE

Marek Szczotka

University of Bielsko-Biała, Faculty of Management and Computer Science, Bielsko-Biała, Poland
e-mail: mszczotka@ath.bielsko.pl

An application of nonlinear optimisation methods to select some parameters of a passenger car steering system is presented. A simplified planar model of the system as well as spatial multibody models are developed. The simplified model is used in the optimisation task, ensuring minimisation of vibrations of the steering wheel. The optimisation task is solved in two stages. The first one allow us to obtain optimal geometry of the system. In the second stage, nonlinear characteristics of some elements are obtained. The correctness of optimisation results is verified by the application of a more sophisticated spatial model. An own simulation programme has been worked out. It allowed us to perform dynamic analysis of the steering kickback using both simplified and complex structural models as well as to execute a built-in optimisation module.
Asymmetric input forces applied to the wheel centre have been used in the computer simulations. The excitations analysed are typical for a car moving over an obstacle. The work presented concentrates on the steering kickback phenomena, which may strongly influence discomfort perceived by the car driver.

Key words: steering system vibrations, driver's comfort, optimisation, dynamic analysis

1. Introduction

Various commercial simulation tools have been widely applied in the engineering practice and they allow users to model dynamics of almost any mechanical system. Yet many industry companies and research centres still work on their own self-developed models. Such models are usually devoted to specific requirements and they can be better adopted than general simulation packages. Simplified, dedicated models are much faster and can be easily adapted to different applications.

Models presented in the paper enable vibrations of a steering system in a passenger car with the McPherson suspension to be simulated. Impulsive vibrations generated by an obstacle are analysed. The primary objective in this work is to reduce the vibration level of the steering wheel generated by impulsive forces due to an uneven road. Steering vibrations of this kind are known as the steering kickback phenomenon.

The steering kickback problem was described, for example, by Kenji and Massaki (1999). The authors investigated the contribution of force and acceleration components to the tie-rod axial force by the application of individual measurements. The component load method was applied to the steering kickback analysis by Cho (2004). A strong influence of the impact load and kingpin moment on the kickback phenomenon was reported. A few of papers dealt with the wheel shimmy problem. In papers by Pacejka (1973), Sharp and Jones (1980), the results obtained were presented as frequency characteristics and time histories. Some simple dynamical models were used. The results of simulations were compared with empirical transfer functions. Steering wheel vibrations as an effect of the wheel shimmy were discussed also by Dodlbacher (1979), where the author presented a structural model of the suspension and suspension frame mounted by bushings, which took elasto-kinematic properties into account. The commercial package ADAMS was applied in order to examine tire radial stiffness variation, static and dynamic imbalance and belt run-out by Balaramakrishna and Kumar (2009). Interesting results related to steering system vibrations were presented by Groll *et al.* (2006). The authors analysed a control system designed to eliminate periodical vibrations without decreasing the road feedback quality. A multibody model of the suspension was used by Ammon *et al.* (1997), with the *BRIT* tire model. Hydraulic power steering system was described together with experimental verification. Harlecki *et al.* (2004) discussed a dynamic multi-body model, taking dry friction into consideration. An influence of clearance and friction in joints on the vehicle behaviour was shown in Lozia and Zardecki (2002). A spatial suspension models with elastic connectors were presented by Knapczyk and Kuranowski (1986). The results presented indicated the importance of flexible bushing elements. Vehicle subsystems are assembled using bushing joints. The work of Ambrosio and Verissimo (2009) demonstrated the modelling approach and simulation results for the whole vehicle with non-ideal joints represented by bushings.

Optimisation of geometrical parameters in multibody systems was presented by Collard *et al.* (2005). The authors proposed a solution to problems with degenerated constraints due to an ill-conditioned Jacobian matrix when performing the optimisation. Penalisation of the objective function was developed

and successfully applied in several examples. Optimisation of a multibody vehicle steering and suspension system was demonstrated by Bian *et al.* (2003). The steering error was optimised, and the vector of design variables of the system consisted of eleven components. An interesting work, concerning global ride index optimisation was reported in Goncalves and Ambrosio (2003). Flexible, spatial model of the sport car was analysed. The optimisation of ride performance was performed by the summation of weighted accelerations in selected points: seat and back of the driver. The suspension spring stiffness and damping ratio were selected as design variables in the optimisation process. The objective was defined based on a ride comfort index given by ISO 2631 standard. The method was also applied by Goncalves and Ambrosio (2005) to optimise handling performance of the car. Suspension system and a railway vehicle multibody models were considered as examples by Datoussaid *et al.* (2002). Evolutionary strategies were applied in order to minimise the toe angle variations in the first system and stability and comfort problems related to the design of the railway car. The evolutionary methods are less competitive in calculation time, but they provide a global optimum in contrast to the deterministic, gradient-based optimisation methods.

A large number of investigations deal with optimal planning of robot trajectory. For example Jutard-Malinge and Bessonnet (2000) presented optimisation of motion of a robot which transfers an object grasped in motion. An optimisation of motion with end-effector defined trajectory was presented by Galicki and Popowicz (1999), motion transfer time minimisation by Chen (1991), minimisation of electromechanical losses showing the energy saving possibility by Sergaki *et al.* (2002). The cited papers are only a few examples and one could easily find applications of optimisation methods to variety of disciplines.

In this paper, dynamic and multibody analysis is performed in order to evaluate the discomfort caused by vibrations occurring on the steering wheel (steering kickback). The main objective of the paper is to present how optimisation methods can be applied in order to choose geometrical parameters and characteristics of nonlinear elements, which minimise vibrations of the steering wheel. Nonlinear functions of the power assistance system and longitudinal stiffness characteristics of the suspension are optimised in the examples presented. Two optimisation routines are proposed, allowing for a selective optimisation of different types of system parameters and simultaneous optimisation.

The full vehicle model, based on homogenous transformations and joint coordinates, including the steering system was presented in Szczotka and Wojciech (2008). A part of this model (the suspension system with the steering

line) is upgraded in this paper in order to model elasto-kinematic behaviour. Some other modifications are introduced into the tire model. The interaction with an uneven road represented by an obstacle with sharp edges is assumed in the model by the use of approximation functions, similarly to the method given by Paciejka (2002) and Zegelaar (1998).

2. Simplified model of the system

This model should predict, with sufficient accuracy, vibrations on the steering wheel transferred from the road. The system considered (Fig. 1) is defined by main geometry components of the suspension and steering system. It has five degrees of freedom. The whole suspended mass is modelled as a single body with appropriate inertial properties. Flexible connection of the lower control arm to the car body is expressed by spring and damping coefficients c_L, b_L or c_N, b_N, respectively. The desired scrub radius R_{scr} and toe angle variation are defined by the location of points R, L and N as well as angles α, β and γ.

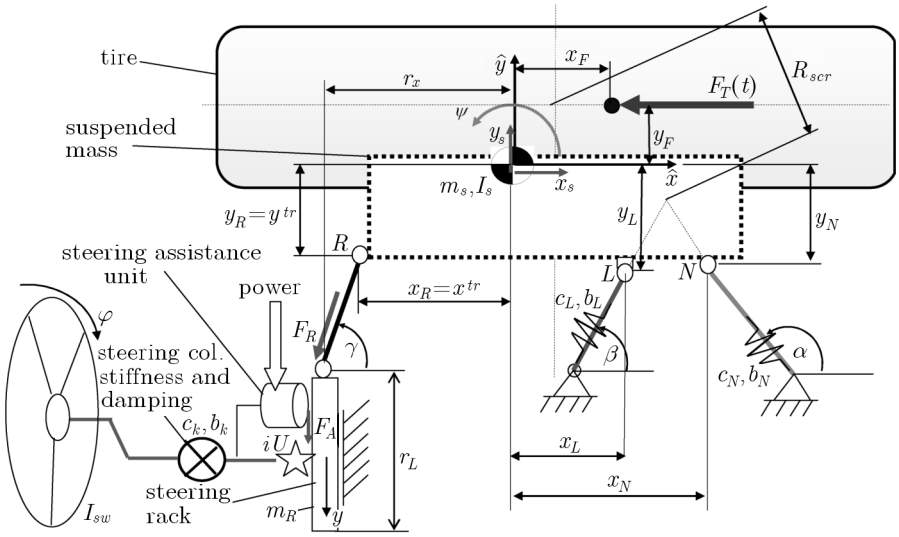

Fig. 1. Simplified model of the steering system

The vector of generalized coordinates $\boldsymbol{q}$ is defined as

$$\boldsymbol{q} = [x_s, y_s, \psi_s, y, \varphi]^\top \tag{2.1}$$

where x_s, y_s are longitudinal and lateral translations of the suspended mass, ψ_s is the rotation angle (small) of the body, y is the displacement of the steering rack, φ is the steering wheel rotation angle.

Force F_R, acting on the steering rack body, can be calculated from its axial deformation, having assumed that

$$F_R = c_R \Delta r = \frac{E_R \pi d_R^2}{4 l_R} \Big([\boldsymbol{r}_0 - \mathbf{T}\boldsymbol{r}_0]^\top [\boldsymbol{r}_0 - \mathbf{T}\boldsymbol{r}_0] \Big)^{\frac{1}{2}} \tag{2.2}$$

where d_R, l_R are the diameter and length of the rod, E_R is the Young modulus of elasticity, and

$$\boldsymbol{r}_0 = [x_R, y_R, 1]^\top \qquad \mathbf{T} = \begin{bmatrix} \cos\psi & \sin\psi & x_s \\ -\sin\psi & \cos\psi & y_s \\ 0 & 0 & 1 \end{bmatrix}$$

x_R, y_R are shown in Figure 1.

The power assistance force F_A is assumed as a function of the steering column deformation or moment applied to the steering wheel. For a hydraulic power assistance system, it can be assumed that

$$F_A = p_A P_{oil}\big(c_k(\varphi - i_U y)\big) \tag{2.3}$$

where p_A is the piston area, $P_{oil} = P_{oil}(M_{sw})$ is the generated pressure (can be a nonlinear function), c_k is the stiffness coefficient of the steering column, i_U is the steering gear ratio.

The equations of motion for this model can be written in the following form

$$\mathbf{M}\ddot{\boldsymbol{q}} + \mathbf{P}\dot{\boldsymbol{q}} + \mathbf{K}\boldsymbol{q} = \boldsymbol{H}(t) \tag{2.4}$$

where $\mathbf{M} = \operatorname{diag}\{m_s, m_s, I_s, m_R, I_{sw}\}$, m_s, I_s are the suspended mass and moment of inertia, respectively, m_R is the steering rack mass, I_{sw} is the steering wheel moment of inertia, $\mathbf{K}$ is the stiffness matrix

$$\mathbf{K} = \begin{bmatrix} \mathbf{K}_s & \mathbf{0} \\ \mathbf{0} & \mathbf{K}_{RS} \end{bmatrix} \qquad \mathbf{K}_s = \begin{bmatrix} c_{1,1} & c_{1,2} & c_{1,3} \\ & c_{2,2} & c_{2,3} \\ \text{sym.} & & c_{3,3} \end{bmatrix}$$

$$\mathbf{K}_{RS} = \operatorname{diag}\{i_U c_{RS}, -c_{RS}\}$$

and

$$
\begin{aligned}
c_{RS} &= c_k(\varphi - i_U y)\\
c_{1,1} &= c_R\cos^2\gamma + c_L\cos^2\beta\\
c_{1,2} &= c_R\sin\gamma\cos\gamma + c_L\sin\beta\cos\beta\\
c_{1,3} &= c_R(x_R\cos\gamma\sin\gamma - y_R\cos\gamma) + c_L(x_L\cos\gamma\sin\gamma - y_L\cos\gamma)\\
c_{2,2} &= c_R\sin^2\gamma + c_L\sin^2\beta\\
c_{3,3} &= c_R(x_R^2\sin^2\gamma + y_R^2\cos^2\gamma - 2x_R y_R\sin\gamma\cos\gamma) +\\
&\quad + c_L(x_L^2\sin^2\beta + y_L^2\cos^2\beta - 2x_L y_L\sin\beta\cos\beta)
\end{aligned}
$$

i_U is the rack gear ratio, $\mathbf{P} = \eta\mathbf{K}$, η is the damping ratio,

$$
\begin{aligned}
\boldsymbol{H}(t) &= [\widetilde{\boldsymbol{H}}^\top, F_R\sin\gamma + F_A(M_{sw}), 0]^\top\\
\widetilde{\boldsymbol{H}} &= \begin{bmatrix} F_N\cos\alpha - F_T(t)\\ F_N\sin\alpha - F_T(t)\\ F_T(t)[y_F - \psi x_F] - F_N(y_b\cos\alpha - x_b\sin\alpha)\end{bmatrix}
\end{aligned}
$$

F_R is defined in (2.2), $F_T(t)$ is the tire contact force due to the road unevenness, $F_A(M_{sw})$ is defined in (2.3), $F_N = F_N(\Delta L, \dot{L})$ is the force due to nonlinear suspension stiffness and damping characteristics.

Having defined the model described by equation (2.4), it is useful to obtain its state-space representation (Kaczorek, 1975). Assuming linearised stiffness and damping characteristics of bushings, equation (2.4) can be rewritten in the following form

$$\ddot{\boldsymbol{q}} = \mathbf{M}^{-1}(\boldsymbol{H} - \mathbf{P}\dot{\boldsymbol{q}} - \mathbf{K}\boldsymbol{q}) \tag{2.5}$$

Denoting the state space vector $\boldsymbol{x}(t) = [\boldsymbol{q}^\top, \dot{\boldsymbol{q}}^\top]^\top$, the full state-space representation takes the form

$$\dot{\boldsymbol{x}}(t) = \mathbf{A}\boldsymbol{x}(t) + \mathbf{B}\boldsymbol{u}(t) \qquad \boldsymbol{y}(t) = \mathbf{C}\boldsymbol{x}(t) + \mathbf{D}\boldsymbol{u}(t) \tag{2.6}$$

where $\boldsymbol{u}(t)$, $\boldsymbol{y}(t)$ are the input and output vectors, and

$$\mathbf{A} = \begin{bmatrix} \mathbf{0} & \mathbf{I}\\ -\mathbf{M}^{-1}\mathbf{K} & -\mathbf{M}^{-1}\mathbf{P}\end{bmatrix} \qquad \mathbf{B} = \begin{bmatrix}\mathbf{0}\\ \mathbf{M}^{-1}\boldsymbol{H}\end{bmatrix} \qquad \mathbf{D} = [\mathbf{0}]$$

matrices $\mathbf{B}$ and $\mathbf{C}$ are defined depending on the input.

Model (2.6) is applied in order to obtain the frequency response of the system. Let us assume the force F_T as the input, and the tie-rod force F_R and steering wheel rotation φ as the outputs. For this case, it can be assumed

$$\mathbf{B} = [0, \ldots, 0, (-\mathbf{M}^{-1}\boldsymbol{H})_1, \ldots, 0]^\top \qquad \mathbf{D} = [\mathbf{0}]$$
$$\boldsymbol{y}(t) = [F_R, \varphi]^\top \qquad \boldsymbol{u}(t) = [1] \tag{2.7}$$
$$\mathbf{C} = \begin{bmatrix} c_R\cos\gamma & c_R\sin\gamma & c_R(y_R\cos\gamma - x_R\sin\gamma) & 0 & 0 & 0 & 0 & 0 & 0 & 0 \\ 0 & 0 & 0 & 0 & 1 & 0 & 0 & 0 & 0 & 0 \end{bmatrix}$$

The main parameters of the steering and front suspension system used in all calculations performed, are listed in Table 1. The presented values are typical for a "C"-segment vehicle.

Table 1. Assumed main parameters of the system

Parameter name	Value
Vehicle speed	35 km/h
Rack friction	0 or 0.08
Suspension / wheel mass	20 kg / 15 kg
Steering column stiffness	60 Nm/rad
Steering wheel inertia	$0.04\,\mathrm{kg\,m^2}$
Ring-rim radial stiffness / damping	$4.5 \cdot 10^7$ Nmm/rad / 5 Nsm/rad
Rack mass	2 kg
Tire belt mass, moment of inertia	15 kg / $0.57\,\mathrm{kg\,m^2}$

Steering wheel tangential acceleration A_{tan} is used in the paper as a parameter describing the vibration level perceived by driver. It is defined as

$$A_{tan} = \ddot{\varphi} r_{sw} \tag{2.8}$$

where $r_{sw} = 185\,\mathrm{mm}$ is the steering wheel radius.

The linear model is used in pre-selection of steering system parameters and in optimisation calculations (in both frequency and time domains). An important property of this model is the simulation time. The time domain analysis of one second of real time takes approx. 50-60 ms, when equations of motion (2.4) are integrated using the Runge-Kutta method of the IV order with the constant time step $h = 10^{-5}$ s. High numerical efficiency is critical for every optimisation problem. All simulations in this and the following sections are performed using an own C++ computer program. Load cases representing a vehicle running over a single obstacle are assumed. Only one side wheel of the vehicle is assumed to pass over the obstacle, generating the kickback phenomenon. The course of the road interaction force can be obtained either from the full vehicle model simulation or from measurements.

3. Optimisation as a tool for reduction of the kickback problem

Steering kickback vibrations are generated as a result of dynamic coupling between vehicle subsystems. Designers have to select many parameters, characteristics and relations in the suspension and steering system. In a complex system, various design criteria have different requirements. Sometimes, it is preferred that the driver "feels" the road by his hands on the steering wheel. At the same time, the driver should be isolated from specific vibrations.

Let us assume that geometrical parameters of the system are components of the vector $\boldsymbol{G}$

$$\begin{aligned} &\boldsymbol{G} = [g_1, \ldots, g_i, \ldots, g_{n_G}]^\top \\ &(\boldsymbol{G}^{min})_i \leqslant (\boldsymbol{G})_i \leqslant (\boldsymbol{G}^{max})_i \qquad \text{for} \quad i = 1, \ldots, n_G \end{aligned} \tag{3.1}$$

where $\boldsymbol{G}^{min}$, $\boldsymbol{G}^{max}$ are minimal and maxiamal acceptable values for geometric parameters, n_G is the number of parameters selected in the optimisation.

Assume also that discrete values of the characteristics which will be optimised are the components of the vector $\boldsymbol{F}$

$$\begin{aligned} &\boldsymbol{F} = [f_0, \ldots, f_i, \ldots, f_{n_F}]^\top \qquad f(s') = SPLINE(s', \boldsymbol{s}, \boldsymbol{F}) \\ &(\boldsymbol{F}^{min})_i \leqslant (\boldsymbol{F})_i \leqslant (\boldsymbol{F}^{max})_i \qquad \text{for} \quad i = 0, \ldots, n_F \end{aligned} \tag{3.2}$$

where $s' = l(t, \boldsymbol{q}, \dot{\boldsymbol{q}})$ is the independent argument of *SPLINE* function which depends on the solution to the equations of motion at time t, $\boldsymbol{s} = [s_0, \ldots, s_{n_F}]^\top$ is the vector of known independent discrete arguments, $f_i = f_i(s_i)$ is the i-th value to be optimised, n_F is the number of discrete points, $SPLINE(\cdot)$ is the 3-rd order spline interpolation function (Fig. 2), $\boldsymbol{q}$ is defined in (2.1), $\boldsymbol{F}^{min}$, $\boldsymbol{F}^{max}$ are minimal and maximal values of the vector $\boldsymbol{F}$.

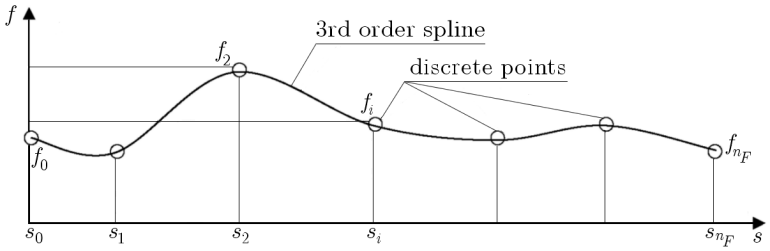

Fig. 2. Discrete representation of a curve by a spline function

Moreover, it is assumed that other design parameters of the system, which are selected at the beginning, remain constant during the optimisation (such as masses, other constrained geometrical parameters), form the vector $\boldsymbol{P}_C$

$$\boldsymbol{P}_C = [P_{C_{(i)}}, \ldots, P_{C_{(n_{PC})}}]^\top \tag{3.3}$$

Two strategies of optimisation are proposed, see Fig. 3. In the first approach, the optimisation is performed in two stages. First, the optimisation task is executed in order to select the set of geometrical parameters of steering and suspension systems. One may find, for example, an optimal location of the steering rack, coordinates of mounts and even mass or moment of inertia. In addition to selection of decision variables (which are components of the vector $\boldsymbol{G}$), all necessary constraints should be provided. When this optimisation task is solved, the solution vector $\boldsymbol{G}^{opt}$ contains the optimal values which are assigned as the system geometry parameters. In the second phase, one performs optimisation of other components, like stiffness characteristics, power assistance characteristics, etc. and the decision variables $\boldsymbol{F}$ represent a discrete function (or several functions). The second approach consists in solving the optimisation task for two decision vectors $\boldsymbol{G}$ and $\boldsymbol{F}$ simultaneously.

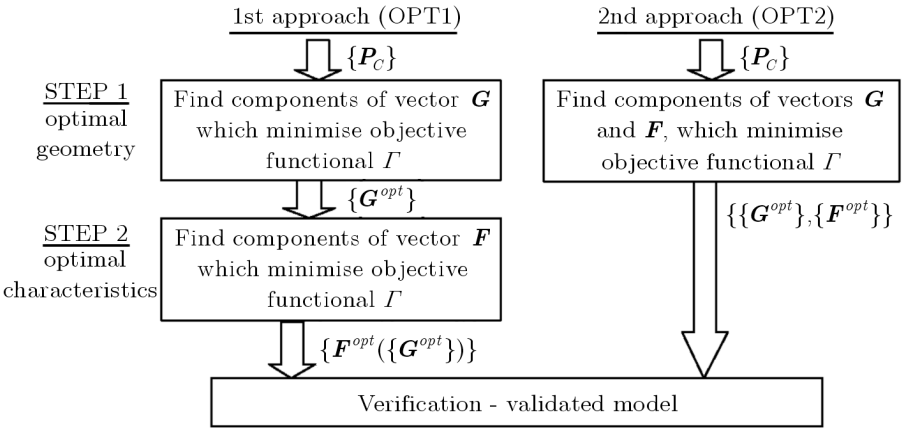

Fig. 3. Two optimisation approaches

The solution of the optimisation problem is defined as follows. Find the minimum of the functional:

$$\Gamma(t, \boldsymbol{q}, \dot{\boldsymbol{q}}, \boldsymbol{X}) \tag{3.4}$$

assuming the decision vector $\boldsymbol{X}$ as

$$\boldsymbol{X} = \begin{cases} \boldsymbol{G} & \text{for} \quad \text{OPT1, STEP 1} \\ \boldsymbol{F} & \text{for} \quad \text{OPT1, STEP 2} \\ [\boldsymbol{G}^{\top}, \boldsymbol{F}^{\top}]^{\top} & \text{for} \quad \text{OPT2} \end{cases} \tag{3.5}$$

with constraint conditions

$$\begin{aligned} d_j(t, \boldsymbol{q}, \dot{\boldsymbol{q}}, \boldsymbol{X}) &\leqslant 0 \qquad \text{for} \quad j = 1, \ldots, n_d \\ e_j(t, \boldsymbol{q}, \dot{\boldsymbol{q}}, \boldsymbol{X}) &= 0 \qquad \text{for} \quad j = 1, \ldots, n_e \end{aligned} \tag{3.6}$$

where n_d, n_e are the numbers of constraint relations (defined by $(3.1)_2$ and $(3.2)_3$).

Calculation of the functional Γ as well as constraints $\boldsymbol{d}$ and $\boldsymbol{e}$, requires equations of motion of the system (2.4) to be integrated in the range of time 0-T. The initial value problem to be solved, rewriting (2.4), is defined by the equations

$$\mathsf{M}\ddot{\boldsymbol{q}} = \boldsymbol{F}(t, \boldsymbol{q}, \dot{\boldsymbol{q}}, \boldsymbol{Y}) \qquad \boldsymbol{q}_{t=0} = \boldsymbol{q}^{(0)} \qquad \dot{\boldsymbol{q}}_{t=0} = \dot{\boldsymbol{q}}^{(0)} \tag{3.7}$$

where $\boldsymbol{q}^{(0)}$, $\dot{\boldsymbol{q}}^{(0)}$ are initial displacements and velocities, respectively, and $\boldsymbol{Y}$ is defined as follows

$$\boldsymbol{Y} = \begin{cases} [\boldsymbol{P}_C^{\top}, \boldsymbol{X}^{\top}, \boldsymbol{0}]^{\top} & \text{for stage OPT1, STEP 1} \\ [\boldsymbol{P}_C^{\top}, \boldsymbol{G}^{opt^{\top}}, \boldsymbol{X}^{\top}]^{\top} & \text{for stage OPT1, STEP 2} \\ [\boldsymbol{P}_C^{\top}, \boldsymbol{X}^{\top}]^{\top} & \text{for the approach OPT2} \end{cases} \tag{3.8}$$

The optimisation problem described can be solved using any optimisation method. In the programme developed, Nelder-Mead's method (proposed in Nelder and Mead, 1965) is implemented and applied. The dynamic equations of motion have to be integrated in every iteration.

3.1. Definition of the objective function

The definition of objective function (3.4) is related to the level of steering wheel vibrations. It is composed of several elements, each of which defines an objective "measure" representing discomfort related to the steering wheel vibrations. The sum of components is assumed to be the objective function

$$\Gamma = \sum_{k=1}^{n_\Gamma} \epsilon_k \widetilde{\Gamma}_k(t, \boldsymbol{q}, \dot{\boldsymbol{q}}, \boldsymbol{X}) \tag{3.9}$$

where $\widetilde{\Gamma}_k = \Gamma_k/\Gamma_k^0$, $\Gamma_k(t, \boldsymbol{q}, \dot{\boldsymbol{q}}, \boldsymbol{X})$ is the k-th component of the vibration "measure" of the steering wheel, $\Gamma_k^0(t, \boldsymbol{q}, \dot{\boldsymbol{q}}, \boldsymbol{X}^{init})$ is the k-th objective function component for initial vector $\boldsymbol{X}^{init}$, n_Γ is the number of vibration "measures", ϵ_k is the k-th weight coefficient.

The selection of functionals Γ_k is described below. Γ_1 equals to the peak-to-peak value of the calculated acceleration signal. The peak-to-peak is especially important when impulsive vibrations with considerable amplitudes are present

$$\Gamma_1 = |\max(\ddot{\varphi}) - \min(\ddot{\varphi})| \tag{3.10}$$

The vibration energy correlated with impulsive, non stationary signal may be described by the component Γ_2 which reflects a change in the vibration level. The component Γ_2 is defined as follows

$$\Gamma_2(t) = \int_0^{\top} \sqrt{\frac{\Gamma_2'(t)}{\Delta t_w}}\, dt \tag{3.11}$$

where

$$\Gamma_2'(t) = \int_{t-\frac{1}{2}\Delta t_w}^{t+\frac{1}{2}\Delta t_w} |\ddot{\varphi}(\tau)|^2\, d\tau$$

and Δt_w is a "moving" time window whose length depends on the vehicle speed (for 35 km/h it can be assumed $\Delta t_w = 0.6$ s), T is the simulation time ($T = 1$ s).

The third component of functional (3.9), Γ_3, describes how different parts of the human body perceive the vibration in different directions. For driver's hands on the steering wheel, one can use the function $W(f)$ presented in Fig. 4a

$$\Gamma_3 = \sqrt{\int_{f_1}^{f_2} |FFT(f)W(f)|^2\, df} \tag{3.12}$$

where $FFT(f)$ is the amplitude of the fast Fourier transformation performed on $\ddot{\varphi}$ at frequency f, f_1, f_2 are the upper and lower limit of frequencies, $W(f)$ is the filter function.

Another objective component is the dissipation time. Let us assume that the excitation intensity rises above some level at time t_1. Then we record

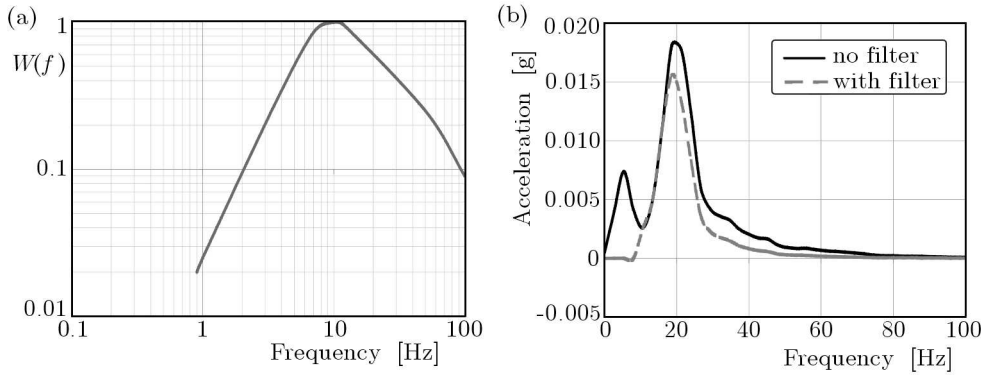

Fig. 4. (a) Function $W(f)$ according to (BS6841, 1987), (b) steering wheel vibration with and without filter

time t_2, when the oscillation energy returns back to the same level observed at time t_1. Therefore

$$\Gamma_4 = T_{DS} \tag{3.13}$$

where $T_{DS} = t_2 - t_1$ is the time period when $\Gamma_2' \geqslant \kappa_{DS} \times \max(\Gamma_2')$, $\kappa_{DS} = 0.25$.

The root mean square is commonly used parameter describing energetic content of a signal. Thus, the last component included in the objective function, is

$$\Gamma_5 = \sqrt{\frac{\int\limits_{T_1}^{T_2} |\ddot{\varphi}(t)|^2 \, dt}{T_2 - T_1}} \tag{3.14}$$

where T_1, T_2 are time intervals (all load cases: $T_1 = 0\,\mathrm{s}$, $T_2 = 1\,\mathrm{s}$).

Some other functions can also be defined. Weight coefficients applied to each component Γ_k, have been assumed as $\epsilon_k = 1$ for $k = 1, \ldots, 5$. The definition of objective function (3.9) allows us to define a single value for the "quality" of a design with respect to the vibration level. Since each component Γ_k is scaled taking the initial value, when assuming the same value for every weight factor ϵ_k, one obtains the same contribution to the objective function. Of course selection of ϵ_k is arbitrary, and one can perform experiments with other values, but the choice made in this work proved the optimisation task to be quite effective. Having introduced a single value as the objective function (also suggested in standards, for example (ISO2631, 1974), most common optimisation routines can be applied in general practical problems. An alternative would be a more complex, multicriteria optimisation method which could compromise several, even conflicting criteria at time.

3.2. Approach OPT1, STEP 1 – geometry optimisation

In this section, we consider that some selected parameters which describe the system geometry can be changed in the optimisation task. The scope of these changes is defined individually for each variable, depending on the specific vehicle model and project limitations. These criteria can be very complex in practice, since a change of any geometric parameter affects other characteristics of the car such as handling, stability, dynamics, safety.

However, in certain situations, the designer may have greater freedom in choosing the basic steering geometry. Then applying the proposed method, he can find an optimal geometry of the system. The parameters of the system, which have been chosen as the decision variables are specified below (shown also in Fig. 1)

$$\boldsymbol{G}_1 = [r_L, r_X, x^{tr}, y^{tr}]^\top \tag{3.15}$$

where r_L is the rack length, r_X is the position of the steering rack, x^{tr} and y^{tr} are the coordinates of the tie-rod spherical joint connecting it with the unsprung mass.

Characteristics of the power assistance system (a) and the longitudinal stiffness of the suspension (b), which are components of the vector $\boldsymbol{F}$, are shown in Fig. 5. These characteristics do not change during the optimisation.

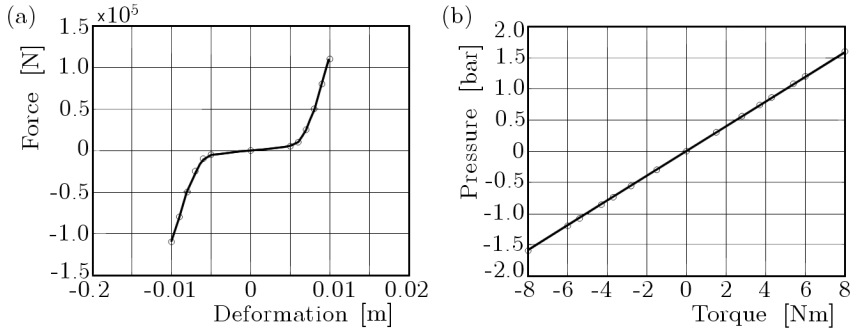

Fig. 5. (a) Stiffness characteristics in the X direction, (b) course of power assistance

The constraint vectors given below allow for a large spectrum of parameter modifications, especially for the steering rack position r_X [m]

$$\begin{aligned} \boldsymbol{G}_1^{min} &= [0.2, -1.3, -0.1825, -0.0725]^\top \\ \boldsymbol{G}_1^{max} &= [0.4, 0.7, -0.0825, 0.0225]^\top \end{aligned} \tag{3.16}$$

As the starting point, the following set of parameters has been assumed ([m])

$$\boldsymbol{G}_1^0 = [0.25, 0.3, -0.1325, -0.025]^\top \tag{3.17}$$

Table 2 and Fig. 6 present the results of geometry optimisation of the system. The left part of Table 2 indicates components Γ_k, before and after optimisation. The ratio $\Gamma^{init}/\Gamma^{opt}$ reflects the magnitude of the change (improvement) of steering wheel vibration in the optimal solution with respect to the initial value. The comparison shows that the peak-to-peak value decreased more than eight times and the dissipation time is almost a half of the initial value. In the right side part, the optimal values of decision variables are listed. The differences between steering acceleration courses are shown in Fig. 6a. The acceleration is almost completely eliminated. Similarly, comparing the results in the frequency domain, a significant reduction of the amplitude $|X(f)|$ has been achieved (Fig. 6b).

Table 2. Results of geometry optimisation case (1), stage OPT1, STEP 1

Component Γ_k	Initial values	Optimal values	Ratio $\Gamma^{init}/\Gamma^{opt}$	Variable	Initial values	Optimal values
Γ_1	39518.2	4574.88	8.638	r_L	0.25	0.219926
Γ_2	2786.27	217.96	12.783	r_X	0.3	−0.243438
Γ_3	68.819	0.607	113.29	x^{tr}	−0.1325	−0.162729
Γ_4	0.863	0.452	1.907	y^{tr}	−0.025	−0.0154482
Γ_5	3079.05	276.805	11.123			

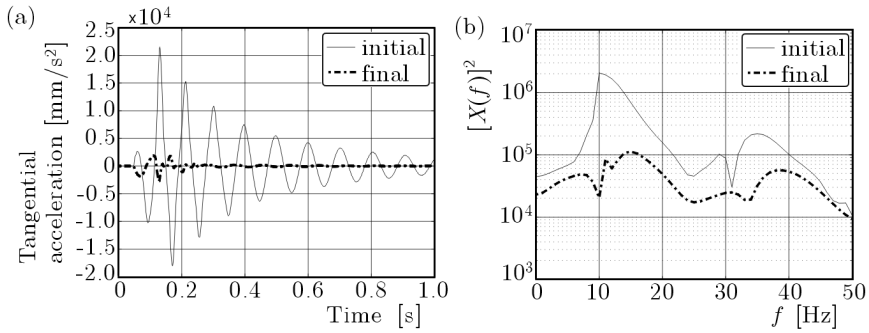

Fig. 6. Stage OPT1, STEP 1, case (1), geometry optimisation (a) time courses of the initial and optimal steering wheel acceleration, (b) frequency spectrum of the tangential acceleration

Such an improvement of the vibration level shown in Fig. 6 is not always possible. Changing the system parameters, for example the steering rack location, can be much limited. In the next example, the variable r_X can vary only in the range of $\pm 5\,\mathrm{cm}$ from its initial position $r_{X_{init}} = 0.05\,\mathrm{m}$. Additionally, we assume that $y^{tr} = -0.025\,\mathrm{m} = \mathrm{const}$.

The results for this case are summarised in Fig. 7 and Table 3. The effect of optimisation is not as spectacular as before. However, the improvement is significant: about 30% reduction of the peak-to-peak steering wheel acceleration is noticeable (Fig. 7a). The obtained level of improvement affects comfort perceived by the driver, see Fig. 7b.

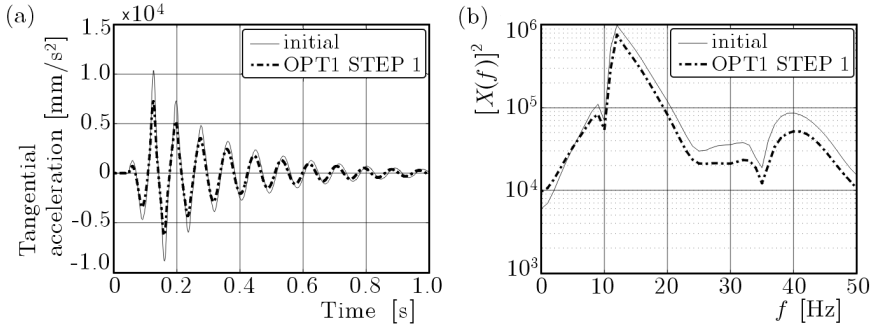

Fig. 7. Stage OPT1 STEP 1, case (2), optimisation of geometry (a) time courses of the initial and final acceleration, (b) frequency spectrum

Table 3. Results of geometry optimisation case (2), stage OPT1, STEP 1

Component Γ_k	Initial values	Optimal values	Ratio $\Gamma^{init}/\Gamma^{opt}$	Variable	Initial values	Optimal values
Γ_1	19243.9	13520	1.423	r_L	0.25	0.2
Γ_2	1188.88	866.91	1.371	r_X	0.05	0.00
Γ_3	14.277	7.602	1.877	x^{tr}	−0.1325	−0.0825
Γ_4	0.748	0.746	1.002	y^{tr} (locked)	−0.025	−0.025
Γ_5	1369.07	998.77	1.371			

3.3. Approach OPT1, STEP 2 – optimisation of characteristics

Having performed the optimisation of geometry, further reduction of the vibration level can be done through the choice of some characteristics of the system. In this section, optimisation of the steering assistance curve and the suspension longitudinal stiffness characteristic is performed. To this end, the

optimal set of parameters $\boldsymbol{G}^{opt}$, chosen in the previous section ("Optimal values", Table 3), is the starting point. The optimisation results are presented in Table 4 and Fig. 8.

Table 4. Results for optimisation stage OPT1, STEP 2

Parameter	OPT1 STEP 1	OPT1 STEP 2	$\frac{\Gamma^{OPT1-STEP1}}{\Gamma^{OPT1-STEP2}}$
Γ_1	13520	9333.02	1.448
Γ_2	866.91	736.38	1.177
Γ_3	7.602	5.322	1.428
Γ_4	0.746	0.764	0.977
Γ_5	998.77	840.99	1.187

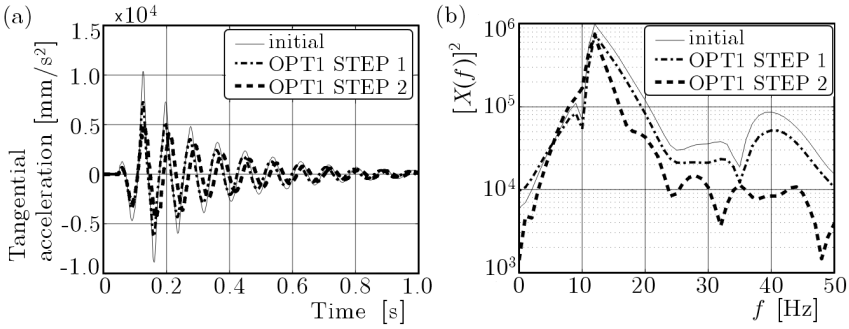

Fig. 8. Results of OPT1 STEP 2 optimisation (a) steering wheel tangential acceleration, (b) frequency spectrum of the steering wheel tangential acceleration

The effectiveness of different approaches to the optimisation problem can be compared by introducing the vibration index I_V, defined as

$$I_V = \sum_{k=1}^{n_\Gamma} \epsilon_k \frac{\Gamma_k^{opt}}{\Gamma_k^{init}} \tag{3.18}$$

where Γ_k^{init}, Γ_k^{opt} values of the objective function components before and after the optimisation, $I_V^{(0)} = \sum_{k=1}^{n_\Gamma} \epsilon_k$ ($I_V^{(0)} = 5$ in all cases considered).

The reduction of the index I_V reached is more than 18.4% (from $I_V^0 = 5.0$ to $I_V^{opt} = 4.081$) compared to the level of vibrations after OPT1 STEP 1. Those results have been obtained, as indicated previously, only by the modification of selected characteristics of the system, without changing the geometry itself. The solution has been obtained after 4332 iterations.

3.4. Second approach: OPT2 – simultaneous optimisation

In this section, all parameters are optimised simultaneously (both vectors $\boldsymbol{G}$ and $\boldsymbol{F}$). The geometry given in Table 3, with identical constraints as specified in Section 3.2 (the second set of parameters) is assumed as the starting point.

The differences between the two approaches are presented in Table 5. Obviously, the first approach (OPT1) allows one to obtain the solution faster. It is much easier to solve two smaller optimisation tasks with n_G and n_F decision variables instead of one large with n_G+n_F variables. Moreover, the result of OPT1 approach is marginally better due to lower I_V. The optimisation method used stops at the local minimum. This local minimum can be different than that obtained in OPT1 step. The system is also very sensitive to geometry changes, and the simultaneous optimisation of selected design variables results in slightly different parameters: $r_L = 0.200057\,\mathrm{m}$, $r_X = 3.50103 \cdot 10^{-8}\,\mathrm{m}$, $x^{tr} = -0.0826746\,\mathrm{m}$.

Table 5. Comparison between simultaneous and successive optimisation

Component Γ_k	OPT2	OPT1 STEP 2	Difference [%]	OPT1 STEP 1
Γ_1	9393	9333.02	0.64	13520
Γ_2	736.42	736.38	0.005	866.91
Γ_3	5.315	5.322	−0.132	7.602
Γ_4	0.765	0.764	0.13	0.746
Γ_5	840.71	840.99	−0.033	998.77
No. of iterat.	6037	4332		192
CPU time	450 s	310 s		15.8 s

The results show that the level of vibration reduction as well as global minima are very similar in both approaches. Both optimisation routines terminate at approximately the same point.

4. Spatial model of the system – indirect verification

The calculation results presented previously have been obtained from a simplified model described in Section 2. In order to prove correctness of the results, an indirect verification is performed. The calculation results are compared with those obtained from a different, more sophisticated and validated model. The spatial model has been verified by road measurements, also during obstacle

passing manoeuvres. An acceptable correspondence of calculations and measurements was achieved, see Szczotka and Wojciech (2008). The rigid finite element method Wittbrodt (2006) was applied in order to discretise flexible links.

The equations of motion of the system with constraints are formulated in the form

$$\mathbf{M}\ddot{\boldsymbol{q}} - \mathbf{D}\boldsymbol{R} = \boldsymbol{F} \qquad -\mathbf{D}^{\top}\ddot{\boldsymbol{q}} = \boldsymbol{G} \tag{4.1}$$

where

$$\boldsymbol{q} = [\boldsymbol{q}_1^{\top}, \ldots, \boldsymbol{q}_{n_B}^{\top}, \boldsymbol{q}_{sl}^{\top}, \boldsymbol{q}_{sr}^{\top}, \boldsymbol{q}_l^{\top}, q_{LT}, q_{RT}]^{\top}$$

and n_B is the number of rigid bodies in the system, $\boldsymbol{q}_i^{\top} = [q_1^{(i)}, \ldots, q_{n_q^{(i)}}^{(i)}]^{\top}$ is the number of generalized coordinates of the body i, $\boldsymbol{q}_{sl} = [q_1^{(sl)}, \ldots, q_{n_{sl}}^{(sl)}]^{\top}$, $\boldsymbol{q}_{sr} = [q_1^{(sr)}, \ldots, q_{n_{sr}}^{(sr)}]^{\top}$ are the vectors of left and right flexible drive axle, n_{sl}, n_{sr} are the numbers of rigid finite elements in the discretisation, $\boldsymbol{q}_l = [q_1^{(l)}, \ldots, q_{n_l}^{(l)}]^{\top}$ is the vector of generalized coordinates of the steering column, $n_l^{(l)}$ is the number of rigid finite elements of the steering column, q_{LT} and q_{RT} are the carcass compliances (used in the tire slip model), $\boldsymbol{R}$ is the vector of unknown constraint reactions

$$\boldsymbol{R} = [\boldsymbol{R}_{J_1}^{\top}, \ldots, \boldsymbol{R}_{J_4}^{\top}, R_Y, M_{DL}, M_{DR}, M_W^{(sl)}, M_W^{(sr)}, F_f]^{\top}$$

and $\boldsymbol{R}_{J_i} = [R_1^{(J_i)}, R_2^{(J_i)}, R_3^{(J_i)}]^{\top}$ is the i-th spherical joint reaction vector, R_Y is the reaction force in the rack-pinion joint, M_{DL}, M_{DR} are reaction torques on differential outputs, $M_W^{(sl)}$, $M_W^{(sr)}$ are reaction torques coupling the driven wheels with drive axles, F_f is the unknown dry friction force, $\mathbf{M}$ is the mass matrix

$$\mathbf{M} = \operatorname{diag}\{\mathbf{M}^{(S)}, \mathbf{M}^{(sl)}, \mathbf{M}^{(sr)}, \mathbf{M}^{(l)}, m_{TL}, m_{TR}\}$$

and $\mathbf{M}^{(S)}$ is the mass matrix of the rigid body system, $\mathbf{M}^{(sl)}$, $\mathbf{M}^{(sr)}$, $\mathbf{M}^{(l)}$ are diagonal mass matrices of flexible shafts, m_{LT}, m_{RT} are small masses representing the tire carcass, $\boldsymbol{F} = \boldsymbol{F}(t, \boldsymbol{q}, \dot{\boldsymbol{q}})$ is the right side vector, $\mathbf{D}$ is the matrix of constraint coefficients, $\boldsymbol{G}^J$ is the right side vector of constraint equations.

The generation procedure for matrices $\boldsymbol{G}$, $\mathbf{D}$, $\mathbf{M}^{(S)}$ and $\boldsymbol{F}$, in the general case of rigid multibody systems with closed kinematic loops, was presented in detail in Szczotka and Wojciech (2008). If one assumes

$$n_l^{(l)} = n_{sl} = n_{sr} = 0 \tag{4.2}$$

the system considered includes the rigid drive axles and steering column.

The tire model used in the developed simulation software is in principle similar to the SWIFT model (Pacejka, 2002; Zegelaar, 1998; Schmeitz *et al.*, 2007). An important advantage of the model is that the tire structural vibrations are taken into account. Usually, natural frequencies of in-plane belt vibrations are in the range of 45-75 Hz.

The results (tangential accelerations) obtained from the spatial model are compared with those from the simplified model used for the optimisation, see Fig. 9. Calculations were carried out for two sets of parameters according to Table 2: initial and optimal. In both cases, a good compatibility of the results has been achieved.

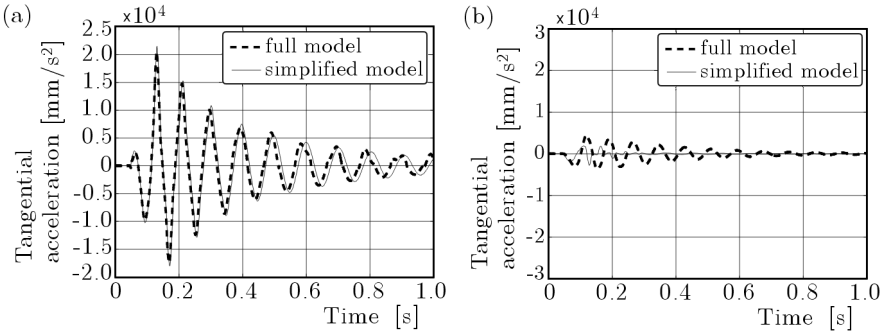

Fig. 9. Comparison of the results: corresponding to the "full" and "simple" model, (a) tangential acceleration of the steering wheel before optimisation, (b) accelerations after application of the optimised characteristic of the steering assistance system

5. Conclusion

The optimisation allowed us to significantly reduce the steering kickback phenomenon. The dynamic analysis of the planar simplified model is useful at the early project stages. It requires only a few basic parameters to be specified. The spatial (full) model requires the complete set of the input data. Obviously, it offers a much wider spectrum of the results and types of analysis. Detailed suspension geometry, mass distribution, stiffness of the components, and many other effects can be reflected. However, due to much longer simulation time, its application to optimisation problems is limited.

The approach proposed, combining two levels of optimisation, can be applied in practice. At the beginning of the design process, there is always some space for changes. The steering-suspension geometry has quite large influence on the steering kickback. Therefore, at the first stage, the geometry of the sys-

tem can be optimised. Having optimised the geometry, optimal characteristics of selected components can be found. It has been shown that it is much easier and faster to optimise components sequentially. In addition, such an approach gives better control of the process.

One of the important features of the models presented is the numerical effectiveness. Simpler models can be easily adapted to special applications (i.e. implemented as modules in the in-house standards transformed to PLC systems). This is of special importance when an optimisation process has to be performed. The software tool developed can be applied in the early design of a steering system, for prediction of the NVH characteristic and other indexes. Having implemented all analysis methods, modules and mathematical models within one software, the user can perform many numerical experiments pretty easy and efficiently.

Acknowledgements

This work has been partially supported by the Polish Ministry of Science and Higher Education within the project No. N502 464934.

References

1. Ambrosio J., Verissimo P., 2009, Improved bushing models for general multibody systems and vehicle dynamics, *Multibody Syst. Dyn.*, **22**, 341-365
2. Ammon D., Gipser M., Rauh J., Wimmer J., 1997, High performance system dynamics simulation of the entire system tire-suspension-steering-vehicle, *Vehicle System Dynamics*, 27, 435-455
3. Balaramakrishna N., Kumar R.K., 2009, A study on the effect of different tyre imperfections on steering wheel vibration, *Vehicle System Dynamics*, **47**, 6, 753-770
4. Bian X.L., Song B.A., Becker W., 2003, The optimisation design of the McPherson strut and steering mechanism for automobiles, *Forschung im Ingenieurwesen*, **68**, 60-65
5. BS6841, 1987, Guide to measurement and evaluation of human exposure to whole-body mechanical vibration and repeated shock, *British Standards Institution*
6. Chen Y.C., 1991, Solving robot trajectory planning problems with uniform cubic B-splines, *Optimal Control Appl. Methods*, **12**, 247-262
7. Cho Y., 2004, Simulation of steering kickback using component load method, *2004-01-1097*, SAE

8. COLLARD J.-F., FISETTE P., DUYSINX P., 2005, Contribution to the optimization of closed-loop multibody systems: application to parallel manipulators, *Multibody System Dynamics*, **13**, 1, 69-84

9. DATOUSSAID S., VERLINDEN O., CONTI C., 2002, Application of evolutionary strategies to optimal design of multibody systems, *Multibody System Dynamics*, **8**, 393-408

10. DODLBACHER G., 1979, Mathematical investigation to reduce steering wheel shimmy, *Vehicle System Dynamics*, **8**, 2, 86-90

11. GALICKI M., POPOWICZ K., 1999, Time-optimal motions of robotic manipulators with end-effector path constraints, *Tenth World Congress on the Theory of Machines and Mechanisms*, Oulu, Finland, 1073-1078

12. GONCALVES J.P.C., AMBROSIO J.A.C., 2003, Optimization of vehicle suspension systems for improved comfort of road vehicles using flexible multibody dynamics, *Nonlinear Dynamics*, **34**, 113-131

13. GONCALVES J.P.C., AMBROSIO J.A.C., 2005, Road vehicle modeling requirements for optimization of ride and handling, *Multibody System Dynamics*, **13**, 3-23

14. GROLL M. VON, MUELLER S., MEISTER T., TRACHT R., 2006, Disturbance compensation with a torque controllable steering system, *Vehicle System Dynamics*, **44**, 4, 327-338

15. HARLECKI A., ADAMIEC-WOJCIK I., KUBAS K., 2004, Dynamic analysis of the steering system of a passenger car with McPherson suspension, *The Archive of Mechanical Engineering*, **LI**, 2, 181-213

16. ISO2631, 1974, Guide for evaluation of human exposure to whole body vibration, *International Organisation for Standardisation*

17. JUTARD-MALINGE A.-D., BESSONNET G., 2000, Optimal motion planning of robotic manipulators removing mobile objects grasped in motion, *Journal of Intelligent and Robotic Systems*, **29**, 233-255

18. KACZOREK T., 1975, *Synthesis of Linear Stationary Systems by the State-Space Method*, PWN, [in Polish]

19. KENJI K., MASSAKI M., 1999, Dynamic analysis on the cause of steering kickback. Part 3. Analyses on transient vibration of unsprung mass by means of force measurement on running vehicle, *Proceedings of JSAE Annual Congress*, **107**, 99, 21-24

20. KNAPCZYK J., KURANOWSKI A., 1986, Analysis of the characteristics of the MacPherson suspension taking silentblocks flexibility into consideration, *The Archive of Mechanical Engineering*, **33**,

21. LOZIA Z., ZARDECKI D., 2002, Vehicle dynamics simulation with inclusion of freeplay and dry friction in steering system, *SAE*, 2002-01-0619

22. Nelder J.A., Mead R., 1965, A simplex method for function minimization, *The Computer Journal*, **7**, 4, 308-313

23. Pacejka H.B., 1973, Approximate dynamic shimmy response of pneumatic tyres, *Vehicle System Dynamics*, 2, 49-60

24. Pacejka H.B., 2002, *Tyre and Vehicle Dynamics*, SAE, Warrendale

25. Schmeitz A.J.C., Besselink I.J.M., Jansen S.T.H., 2007, TNO MF-SWIFT, *Vehicle System Dynamics*, **45**, 1, 121-137

26. Sergaki E.S.S., Stavrakakis G.S., Pouliezos A.D., 2002, Optimal robot speed trajectory by minimization of the actuator motor electromechanical losses, *Journal of Intelligent and Robotic Systems*, **33**, 187-207

27. Sharp R.S., Jones C.J., 1980, A comparison of tyre representations in a simple wheel shimmy problem, *Vehicle System Dynamics*, 9, 45-57

28. Szczotka M., Wojciech S., 2008, Application of joint coordinates and homogenous transformations to modeling of vehicle dynamics, *Nonlinear Dyn.*, **52**, 377-393

29. Wittbrodt E., Adamiec-Wojcik I., Wojciech S., 2006, *Dynamics of Flexible Multibody Systems. Rigid Finite Elements*, Springer-Verlag

30. Zegelaar P.W.A., 1998, *The dynamic response of tires to breake torque variations and road unevennesses*, TU Delft

Symulacja i optymalizacja drgań typu *kickback* koła kierownicy samochodu

Streszczenie

W pracy przedstawiono zastosowanie metod optymalizacji do doboru pewnych parametrów układu kierowniczego samochodu osobowego. Przedstawiono zarówno uproszczony, płaski model układu, jak również jego wersję przestrzenną. Model uproszczony wykorzystano w zadaniach optymalizacji, których celem jest minimalizacja drgań przenoszonych na koło kierownicy w wyniku jazdy po nierównej nawierzchni. Zadanie optymalizacji jest rozwiązane w dwóch etapach. W pierszym poszukiwano optymalnej geometrii układu. Nieliniowe charakterystyki układu są znajdywane w drugim etapie. Wyniki optymalizacji zostały następnie zweryfikowane w złożonym modelu układu. Własne oprogramowanie pozwala na przeprowadzanie analiz z zastosowaniem obu modeli oraz dokonywania obliczeń optymalizacyjnych.

Analizowano wpływ sił dynamicznych chrakterystycznych dla przejazdu przez przeszkodę kołami jednej strony pojazdu. Wyniki obliczeń koncentrują się na drganiach typu *kickback*, które są jednym z czynników znacznie wpływających na dyskomfort kierowcy.

Manuscript received April 12, 2010; accepted for print August 16, 2010